島根大学地球資源環境学研究報告　30, 17～24 ページ（2011 年 12 月）
Geoscience Rept. Shimane Univ., 30, p.17～24（2011）

Article

Major and trace element compositions of Devonian and Carboniferous sedimentary rocks from the Tsetserleg terrane, Hangay-Hentey basin, central Mongolia

Narantuya Purevjav* and Barry P. Roser*

Abstract

The Tsetserleg terrane forms part of the Hangay-Hentey basin of Mongolia, which in turn forms part of the Central Asian Orogenic Belt. Whole-rock major and trace elements compositions of 94 Devonian and Carboniferous sandstones and mudrocks (siltstones and mudstones) from the Tsetserleg terrane were determined by X-ray fluorescence spectrometry. Analyses are reported for the Devonian Erdenetsogt (n = 54) and Tsetserleg Formations (n = 26), and the Carboniferous Jargalant Formation (n = 14). The main feature of the data is the relatively uniform average SiO_2 content of the sandstones in each formation. Average SiO_2 contents in the mudrocks are equally uniform, and are only slightly less than those for companion sandstones. Consequently, average concentrations of most of the other elements analyzed are only slightly greater in the mudrocks than in the sandstones. These features reflect the textural and mineralogical immaturity of these sediments, which are classed as wackes and shales based on geochemical parameters.

Key words: Central Asian Orogenic Belt (CAOB), mudstones, sandstones, geochemistry, Tsetserleg terrane, Hangay-Hentey basin, Mongolia

Introduction

The Hangay-Hentey basin is situated in central Mongolia, and forms part of the Central Asian Orogenic Belt (CAOB), the longest-lived and largest Phanerozoic accretionary orogen on Earth. The CAOB is considered to have evolved over 800 Ma, and is characterized by both lateral and vertical growth of the continental crust by accretion of arc, back arc, oceanic islands, seamounts, ophiolitic and Precambrian micro-continental fragments (Jahn *et al*., 2004; Windley *et al*., 2007; Kröner *et al*., 2007; Kelty *et al*., 2008; Lehman *et al*., 2010; Rojas-Agramonte *et al.,* 2011). The CAOB is bounded on the north by Siberian Craton and to the south by the Tarim-North China Craton (Sengör *et al.* 1993; Badarch *et al.* 2002; Long *et al.* 2011). The development of the CAOB is related to complex geological processes, including accretion of island arcs, ophiolites, and subduction units and terranes; the origin of many of these units remains controversial. The tectonic development of Mongolia is genetically related to the CAOB, and thus this is also still a matter of debate (Ruzhentsev *et al*., 1996; Badarch *et al.,* 2002).

The Hangay-Hentey basin (Fig. 1) lies within the northern domain of Mongolia, and is composed of Precambrian and lower Paleozoic metamorphic rocks, Neoproterozoic ophiolites, Lower Paleozoic island arc volcanics, Devonian to Carboniferous sediments and Permian volcanic-plutonic belts, with associated marine and non-marine beds (for details see Badarch *et al*., 2002; Orolmaa *et al*., 2008). In the south the Tsetserleg terrane forms part of the Hangay sub-belt. The Tsetserleg terrane contains the Devonian to Carboniferous Erdenetsogt, Tsetserleg and Jargalant Formations, which are composed of deep marine turbidite to shallow marine sedimentary sequences (Genden *et al*., 2005; Tomurtogoo *et al*., 2006)

Several investigations have been mainly focused on the CAOB in relation to geodynamics and geological processes (Sengör and Natal'in 1996; Jahn *et al*., 2000; Badarch *et al*., 2002; Windley *et al*., 2007; Kelty *et al.* 2008; Long *et al.,* 2011a, b). Some provenance studies have also been carried out mainly based on geochronology (Kelty *et al*., 2008; Long *et al.* 2010; 2011a, b; Ren *et al.* 2011; Rojas-Agramonte *et al.* 2011). However, Long *et al.* (2011a, b) have recently used geochemical compositions of sedimentary sequences to reveal the provenance and weathering histories of Paleozoic greywackes from the Chinese Altai and Junggar blocks. However, similar geochemical investigations of the Devonian-Carboniferous sedimentary sequences of the Hangay-Hentey basin have not yet been made, and the geochemical composition of the sediments and their provenance and tectonic setting of deposition remain obscure.

Previous investigations have noted that the tectonic origin and geodynamics of the Hangay-Hentey basin in relation to the development of the CAOB are still controversial (Sengör *et al.* 1993; Dobrestov *et al.* 1996; Badarch *et al.* 2002; Windley *et al.* 2007; Kelty *et al.* 2008), as reviewed by Lehman *et al.* (2010). However, the recent study by Kelty *et al.* (2008) suggested that the Hangay-Hentey basin developed between island arc systems with a Neoproterozoic basement and an Andean continental margin arc.

Geochemical compositions of sedimentary rock have been used successfully to identify the ancient tectonic settings of depositional basins (Bhatia and Crook 1986; Roser

* Dept. of Geoscience, Shimane University, 1060 Nishikawatsu, Matsue 690-8504, Japan

and Korsch 1986), as recently applied to the Chinese Altai and Junggar blocks of the NW China segment of the CAOB by Long *et al.* (2011a, b). Therefore, the geochemical composition of sedimentary rocks can be used to test the above controversial concept regarding the tectonic origin of the Hangay-Hentey basin in relation to the CAOB. Geochemical data would also help identify source rock composition, crustal evolution, and weathering history in relation to paleoclimate.

Based on the above issues, the purpose of this report is to present major and trace element analyses of Devonian-Carboniferous sandstones and mudrocks from the Tsetserleg terrane. Average concentrations in the two primary lithotypes (sandstones and mudrocks) will also be compared between formations. Comparison of these analyses with existing data from other basins will contribute to our understanding of the complex geological processes and development of the Hangay-Hentey basin in relation to the CAOB. Further interpretation of the data with respect to provenance, tectonic setting and source weathering will be made in a future publication.

Geology

Geologically Mongolia is divided into two parts by the Mongolian Main Lineament (Tomurtogoo 1997; Badarch 2005; Kashiwagi *et al.* 2004; Kelty *et al.* 2008). The Hangay-Hentey basin falls within the northern domain (Badarch *et al.* 2002). The Hangay-Hentey basin was floored by either an enriched mantle or Precambrian basement (Jahn *et al.* 2004; Kelty *et al.* 2008), and is predominantly composed of folded and faulted Devonian to Carboniferous turbidite sequences. These are underlain by Neoproterozoic-Lower Paleozoic shelf carbonate-quartzite sequences and deep marine sediments (Badarch *et al.* 2002), and are intruded or overlain by Mesozoic and Cenozoic igneous rocks (Tomurtogoo *et al.*, 2006; Kelty *et al.* 2008). The present study area is within the Hangay sub-basin of the larger Hangay-Hentey basin. A Cenozoic fault system separates the Hangay and Hentey sub-basins (Badarch *et al.* 2002; Kelty *et al.* 2008; Kurihara *et al.* 2009). The Hangay sub-basin is further divided into several terranes. The Tsetserleg terrane, the object of this study, is one of these (Fig. 1).

The Tsetserleg terrane consists mainly of the Erdenetsogt and Tsetserleg Formations (Devonian) and the Jargalant Formation (Carboniferous). Age has been distinguished based on tabulate coral and brachiopods (e.g. *Neospirifer derjawini*, *Orulgania aff. gumbiniana* Kotf., *Tomiopsis* sp., *Lanipustula* sp., *Dengalosia* sp., *Suleoretepora* sp., *Fenestella* sp., *Fenniretepora* sp,) which lived in marine conditions during the Devonian period (Bayamba *et al.* 1994). Erdenetsogt Formation is composed mainly of grey to green turbidite sandstones, siltstones and mudstones, along with subordinate conglomerates, brown jaspers, and tuffaceous andesites (Kashiwagi *et al.* 2004; Genden *et al.* 2005, 2007; Sambuu *et al.* 2005; Tomurtogoo *et al.,* 2006). Tsetserleg Formation consists mainly of grey sandstones, siltstones and mudstones with occasional conglomerates, interpreted to have been deposited in a marine environment, along with thin layers of andesitic tuff (Tomurtogoo *et al.,* 2006; Kelty *et al.* 2008). Jargalant Formation is composed of grey sandstones, siltstones and mudstones that were also deposited in a marine environment (Genden *et al.* 2005, 2007; Tomurtogoo *et al.,* 2006).

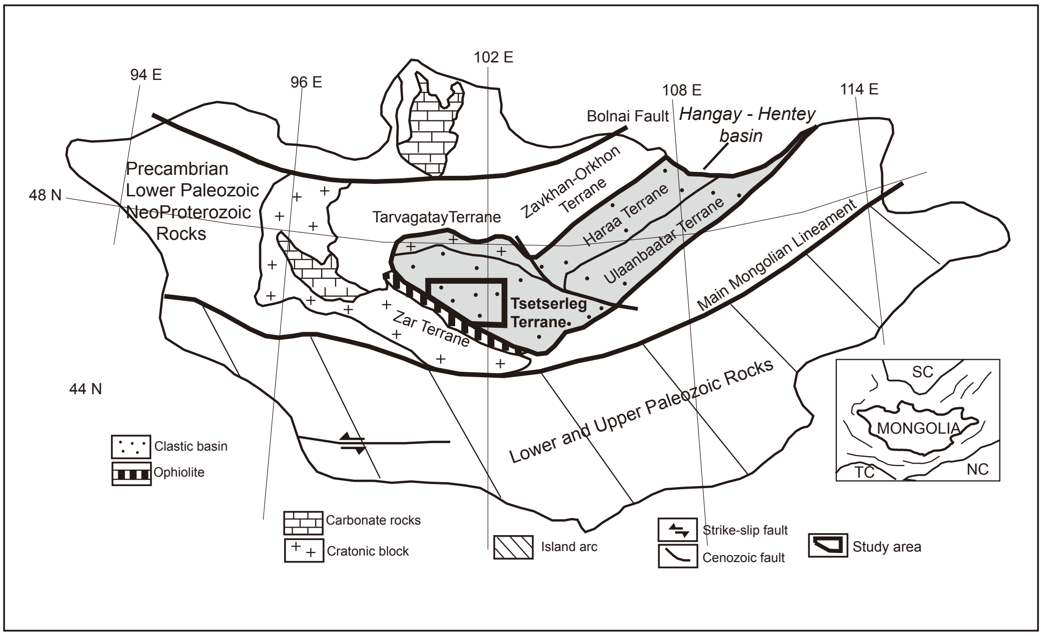

Fig. 1. Distribution of major terranes and structural features in Mongolia, after Badarch *et al.* (2002), Rojas-Agramonte *et al.* (2011) and Wainwright *et al.* (2011), and location of the Tsetserleg terrane and the study area.

Sampling and sample preparation

Field sampling

Ninety-four sandstones and mudrocks (siltstones and mudstones) were collected from outcrops of the three formations, spread over an area of about 500 km^2. Owing to the regional scale of the current mapping, the physical isolation of outcrops from each other, complex structure and limited field time, stratigraphically controlled sampling within individual formations was not feasible. The sample suites should thus be regarded as representative of each formation, within the constraints of current mapping and age control. Fifty-four samples (25 sandstones, 29 mudrocks) were collected from the Erdenetsogt Formation, 26 from the Tsetserleg Formation (11 sandstones, 15 mudrocks), and 14 from the Carboniferous Jargalant Formation (six sandstones, eight mudrocks). Samples were collected only from fresh outcrops. Individual samples weights were generally 200 to 300 g for sandstones and 75 to 150 g for mudrocks.

Sample preparation

Thin weathered surfaces and any veins were removed from samples during manual chipping into 1 to 2 cm pieces using a geological hammer and a manual splitter. The chipped samples (100 g) were placed in Pyrex beakers and washed several times under running tap water and then deionized distilled water to remove surface dust. The samples were then immersed in deionized distilled water, and left to stand for about 24 hours. The samples were then drained, and oven dried at 110° C for 24 hours prior to milling. The samples were crushed using a ROCKLABS model RC ring mill with a 100 g capacity tungsten carbide head. Individual samples were crushed for 25-45 seconds, depending on lithology and sample weight. Splits of the powdered samples (8-10 g) were transferred to glass vials and returned to a 110 °C oven for 24 hours prior to determination of loss on ignition (LOI).

Analytical methods

LOI values were determined by ignition of the dried samples in a muffle furnace at 1020 °C for more than 2 hours. LOI was calculated from the difference between initial weight and the ignited weight of the samples. The LOI values thus include loss of volatiles (e.g. H_2O, F, Cl, CO_2, SO_4) and weight gains through oxidation (conversion of FeO to Fe_2O_3, oxidation of sulfides). The ignited samples were manually disaggregated in an agate pestle and mortar, returned to glass vials, and held in a 110 °C oven before preparation of glass fusion beads for X-ray fluorescence (XRF) analysis.

The XRF analysis was carried out at Shimane University, using a Rigaku RIX 2000 spectrometer fitted with a Rh-anode tube. Major elements and 14 trace elements (Ba, Ce, Cr, Ga, Nb, Ni, Pb, Rb, Sc, Sr, Th, V, Y, Zr) were determined from the glass fusion beads, which were prepared with an alkali flux (80% lithium tetraborate, Merck Spectromelt® A10; 20% lithium metaborate, Merck Spectromelt® A20), in a sample to flux ratio of 2:1 (Kimura and Yamada 1996). Instrument conditions, calibration and corrections for spectral interferences followed the methodology of Kimura and Yamada (1996). Internal correction for intra-run drift was made using secondary calibration against ten Geological Survey of Japan (GSJ) rock standards spanning the compositional range from gabbro (JGb-1) through to granite (JG-2). Four additional trace elements (La, As, Zn, Cu) were determined from pressed powder pellets, using conventional peak over background methods. Calibration was made against seven GSJ rock standards, with concentration ranges for the target elements exceeding those of the samples. Roser *et al.* (1998, 2000, 2003) give additional descriptions of the sample preparation and XRF methodologies used at Shimane University.

Results and Discussion

Major and trace elements analyses (anhydrous normalized basis) of Erdenetsogt, Tsetserleg and Jargalant Formation sandstones and mudrocks are listed in Table 1, along with lithotype averages for each formation. Comparatively small variations in average major and trace element abundances are observed between lithotypes and formations, but these may be significant.

Geochemical compositions of the sediments are the end products of processes acting on the source material during weathering, transport, and deposition, and hence are influenced by the interplay of multiple factors. These processes tend to destroy unstable phases such as feldspar, ferromagnesian minerals, and lithic fragments, converting them to clays, and also passing mobile elements into solution. Concentrations of quartz increase relative to these labile phases if the process continues.

In mature sedimentary successions the major element compositions of the sediments are mainly controlled by the relative proportions of quartz (leading to higher SiO_2) and clays (higher Al_2O_3). As SiO_2 is the dominant major element in siliciclastic sediments, this leads to positive correlation of most other elements with Al_2O_3 as a result of hydrodynamic sorting. However, in less mature sediments the role of lithic fragments can also play a major role in determining bulk chemistry, depending on the proportions of the differing lithic fragments present (e.g. the proportion of mafic or intermediate volcanic lithics to felsic volcanic lithics). Based on geochemical parameters, the Tsetserleg terrane sandstones and shales examined here are classed as wackes and shales, respectively (Purevjav and Roser 2011), and hence are mineralogically immature.

Loss on ignition values in all sandstones and mudstones are low, with only four samples exceeding 5 wt%, and average LOI for both lithotypes in each formation is <3

Table 1. Whole-rock XRF major and trace element XRF analyses of sandstones and mudrocks from theTsetserleg terrane, central Mongolia (anhydrous normalized basis). See footnotes for explanation of abbreviations and treatment of the data.

			Major elements (wt%)										Trace elements (ppm)																			
SaNr	Field No	Lith	SiO_2	TiO_2	Al_2O_3	Fe_2O_3	MnO	MgO	CaO	Na_2O	K_2O	P_2O_5	Ba	Ce	Cr	Ga	Nb	Ni	Pb	Rb	Sc	Sr	Th	V	Y	Zr	La	As	Zn	Cu	Total*	LOI
Erdenetsogt Formation mudrocks																																
HA-4	49/1	Mst	64.09	0.81	17.63	5.81	0.07	1.78	2.22	2.81	4.60	0.18	793	81	25	24	14	12	16	145	14.2	596	12.3	112	28	271	35	3	84	8	99.82	2.18
HA-6	51/1	Zst	66.79	0.68	16.17	4.72	0.06	1.45	1.95	3.51	4.51	0.17	1202	73	9	17	13	5	22	119	8.6	730	12.2	71	24	284	27	7	96	10	99.83	1.68
HA-12	10/1	Zst	66.54	0.70	14.01	6.80	0.05	3.29	4.79	1.35	2.29	0.18	472	61	83	16	12	51	13	88	19.8	146	7.9	120	23	149	24	1	114	25	99.82	6.02
HA-16	12/1	Mst	66.85	0.59	16.49	5.23	0.11	1.44	1.54	3.76	3.58	0.41	783	87	10	24	14	7	19	115	4.3	168	12.8	73	40	257	50	13	141	15	99.59	2.64
HA-20	13/1	Mst	68.09	0.64	15.26	4.92	0.10	1.41	2.02	3.94	3.44	0.18	871	62	6	20	11	5	19	101	14.4	302	8.4	79	32	233	30	5	88	7	99.82	2.18
HA-22	14/1	Zst	70.16	0.52	14.92	3.99	0.09	1.14	1.44	4.14	3.48	0.13	974	61	6	17	10	3	19	86	9.0	264	9.5	60	26	295	24	8	71	2	99.87	1.38
HA-24	15/1	Mst	66.09	0.61	16.55	4.72	0.08	1.70	3.48	2.98	3.62	0.17	603	75	3	24	16	7	25	141	12.0	381	16.5	71	41	211	33	6	109	14	99.83	1.73
HA-29	17/1	Mst	71.89	0.48	14.38	3.21	0.07	0.98	1.77	4.35	2.77	0.11	660	65	9	14	9	4	13	75	8.3	310	9.6	58	24	253	24	6	63	6	99.89	0.93
HA-30	18/1	Zst	68.01	0.59	15.98	4.04	0.08	1.24	2.51	4.14	3.27	0.14	699	78	12	20	11	4	13	95	10.2	445	11.2	71	29	291	30	5	68	6	99.86	1.29
HA-34	21/1	Mst	64.32	0.75	16.78	5.41	0.10	1.97	3.44	3.98	3.06	0.20	556	59	14	22	11	10	13	107	14.2	507	9.6	89	30	180	30	2	97	1	99.80	1.68
HA-37	23/1	Zst	63.36	0.74	16.41	6.72	0.12	2.44	3.43	3.32	3.25	0.21	998	46	24	19	9	12	18	91	11.3	490	8.5	101	24	172	21	3	103	22	99.79	2.14
HA-39	24/1	Mst	62.48	0.78	16.63	6.28	0.13	2.37	3.84	4.26	2.69	0.54	668	61	15	21	11	10	13	77	15.1	511	8.8	104	29	186	33	4	108	22	99.46	2.04
HA-40	28	Mst	64.08	0.79	16.79	7.93	0.17	1.89	0.79	1.80	5.60	0.17	1298	52	34	25	15	55	25	159	22.1	79	13.0	134	28	200	37	1	150	71	99.83	3.00
HA-41	28/1	Mst	63.75	0.79	17.53	7.05	0.17	1.99	0.89	1.63	6.04	0.16	2024	37	33	28	16	63	28	170	20.3	108	13.8	138	29	205	31	3	150	96	99.84	3.74
HA-42	29	Mst	64.71	0.78	18.22	5.22	0.06	1.52	1.43	2.65	5.21	0.20	1128	75	9	21	13	7	16	141	11.2	423	11.9	95	28	298	40	10	113	19	99.80	4.74
HA-49	44/1	Mst	63.73	0.83	18.10	6.71	0.06	2.06	0.62	1.82	5.72	0.37	1237	80	33	25	15	14	21	192	14.4	287	12.1	115	32	269	44	12	118	17	99.63	3.18
HA-51	45/1	Mst	67.52	0.65	16.53	4.84	0.07	1.53	1.28	3.87	3.55	0.16	782	71	19	20	13	10	11	111	8.7	414	10.2	83	25	261	28	4	84	8	99.84	2.31
HA-52	+46/1	Zst	64.15	0.75	17.70	5.74	0.08	1.71	1.64	3.23	4.81	0.19	1038	78	15	23	14	9	15	140	10.7	498	10.8	92	31	271	41	5	94	7	99.81	2.55
HA-53	47/1	Mst	66.76	0.64	16.57	5.22	0.06	1.54	1.35	3.08	4.61	0.17	992	64	17	20	12	6	19	136	9.7	442	9.7	80	23	276	29	6	79	13	99.83	2.23
HA-55	48/1	Zst	62.28	0.90	18.12	6.20	0.08	2.00	2.34	2.55	5.30	0.23	1068	78	31	27	16	13	18	151	12.8	509	13.5	132	33	284	39	3	105	13	99.77	2.66
HA-56	50/1	Zst	66.26	0.70	16.59	5.46	0.11	1.80	1.19	4.60	3.11	0.18	882	64	29	21	13	13	14	95	10.9	308	10.9	98	28	241	42	4	100	10	99.82	1.93
HA-60	54/1	ZSt	65.30	0.70	17.21	5.33	0.12	2.04	1.28	3.73	4.12	0.17	859	76	15	23	15	10	24	142	11.4	357	12.5	83	27	238	40	7	90	31	99.83	2.12
HA-61	55/1	Mst	67.31	0.66	16.51	5.31	0.07	1.47	0.80	4.21	3.47	0.18	866	74	16	18	15	7	17	102	9.5	309	13.6	75	27	308	35	7	82	15	99.82	2.20
HA-63	57/1	Mst	64.22	0.80	17.15	6.09	0.08	1.76	1.97	2.43	5.16	0.33	1034	72	25	25	15	9	21	158	11.0	357	12.1	114	30	256	37	8	100	20	99.67	2.59
HA-73	77/1	Zst	59.55	1.06	21.64	6.02	0.06	1.71	1.37	1.79	6.55	0.26	966	78	39	29	20	20	14	201	15.8	182	15.9	140	32	350	19	6	149	8	99.74	5.05
HA-79	85/1	Mst	55.10	1.16	26.72	4.05	0.04	1.18	0.20	2.49	9.03	0.03	1542	98	21	38	21	5	8	219	19.6	166	9.6	103	42	458	35	92	91	2	99.97	7.63
HA-81	86/1	Mst	73.41	0.36	16.92	2.31	0.06	1.00	0.17	0.20	5.87	0.10	1299	61	2	24	12	4	4	194	6.3	34	9.1	18	32	247	30	1	48	0.2	100.29	3.58
HA-83	87/1	Mst	66.09	0.87	18.92	4.24	0.08	0.78	0.43	4.82	3.59	0.18	705	36	41	21	14	16	11	118	10.1	330	9.9	103	26	273	16	18	79	1	99.82	3.76
HA-127	2511	Mst	68.43	0.65	17.89	4.17	0.04	1.13	0.61	2.32	4.64	0.12	971	68	15	21	15	5	13	139	6.2	256	11.9	76	24	247	26	3	63	12	99.37	3.71
Mudrock average			*65.56*	*0.72*	*17.25*	*5.30*	*0.09*	*1.67*	*1.75*	*3.09*	*4.38*	*0.20*	*964*	*68*	*21*	*22*	*14*	*14*	*17*	*131*	*12.1*	*342*	*11.3*	*93*	*29*	*257*	*32*	*9*	*98*	*17*	*99.80*	*2.86*
Erdenetsogt Formation sandstones																																
HA-1	22/1	Vfsst	62.83	0.87	16.66	6.41	0.12	2.22	3.60	3.92	3.16	0.22	1064	48	20	20	8	8	14	81	17.4	570	6.5	131	23	189	23	4	99	13	99.78	1.67
HA-2	44	Fsst	71.65	0.64	15.03	3.37	0.03	0.96	0.56	4.35	3.24	0.16	913	62	10	16	8	5	19	85	8.8	615	6.6	68	20	217	28	12	72	13	99.47	1.27
HA-7	62	Msst	62.29	0.84	17.35	6.42	0.10	2.26	3.79	3.60	3.09	0.25	725	66	20	21	9	12	17	68	14.8	825	9.0	116	25	210	24	7	103	19	99.27	2.28
HA-8	63	Fsst	61.48	0.85	16.99	6.59	0.10	2.56	4.27	4.08	2.84	0.24	826	56	20	20	9	10	14	73	16.4	384	6.4	115	22	189	24	6	95	17	99.72	1.80
HA-11	10	Msst	72.79	0.75	9.21	4.69	0.09	1.60	7.71	2.02	0.95	0.19	219	78	101	10	11	25	12	43	15.0	187	9.5	93	28	298	30	2	61	24	99.17	6.88
HA-13	11	Vfsst	69.20	0.57	16.73	3.73	0.06	1.38	1.17	4.45	2.62	0.11	1031	76	31	21	12	15	12	84	11.2	394	9.6	65	27	258	26	5	65	3	100.30	2.19
HA-14	11/1	Vfsst	69.88	0.57	15.94	4.07	0.05	1.63	1.12	3.98	2.65	0.11	903	70	33	18	13	13	14	84	12.4	322	9.8	66	28	244	26	8	73	7	99.89	1.98
HA-15	12	Msst	72.72	0.42	14.66	2.69	0.05	0.76	0.98	4.80	2.81	0.11	691	61	2	16	9	1	13	73	8.6	202	7.0	46	23	239	26	7	51	3	99.84	2.44
HA-17	12/2	VFsst	76.03	0.02	14.58	0.64	0.04	0.16	0.25	4.37	3.90	0.00	206	13	2	29	16	2	26	275	4.8	54	11.8	1	2	58	2	3	57	1	99.68	0.81
HA-18	12/3	Vfsst	68.39	0.59	15.85	4.39	0.09	1.22	1.40	4.08	3.76	0.21	974	59	7	23	13	5	17	106	12.3	202	11.4	70	35	271	38	11	98	12	99.79	2.41
HA-19	13	Vfsst	69.85	0.56	14.70	4.04	0.07	1.31	1.82	5.27	2.29	0.10	736	49	10	17	7	3	10	50	11.7	328	7.5	81	20	231	21	8	57	5	100.19	1.54
HA-21	14	Fsst	71.96	0.43	13.91	3.56	0.07	0.99	1.58	4.64	2.78	0.09	641	60	3	17	9	4	15	73	10.7	289	8.9	49	23	267	24	6	63	1	99.67	2.03
HA-23	15	Fsst	70.11	0.44	14.89	3.46	0.07	1.20	2.53	3.80	3.38	0.12	910	56	6	16	10	3	18	96	8.2	340	10.9	50	25	216	22	4	63	7	99.46	0.99
HA-28	17	Msst	70.46	0.52	14.87	3.68	0.08	1.03	2.01	4.00	3.24	0.13	799	64	6	18	10	5	15	87	8.5	314	9.3	63	25	237	27	6	75	6	99.87	1.06
HA-32	20	Msst	68.27	0.53	15.63	4.15	0.07	1.37	2.80	3.86	3.15	0.16	772	54	13	18	9	5	14	92	10.3	401	9.2	69	24	222	19	3	63	9	100.06	1.21
HA-33	21	Fsst	68.60	0.63	15.15	4.49	0.07	1.25	3.12	4.11	2.45	0.13	652	71	19	17	9	6	11	60	11.1	379	9.5	95	23	326	27	3	57	12	99.82	1.16
HA-35	22	Fsst	64.65	0.74	16.07	5.46	0.10	2.15	3.63	4.38	2.61	0.20	609	73	21	18	9	8	13	66	11.1	478	9.3	107	26	261	29	3	80	11	99.81	1.37
HA-36	23	Vfsst	64.44	0.72	16.40	5.49	0.09	2.08	3.83	4.07	2.68	0.19	968	41	20	19	8	11	14	71	15.1	524	7.2	101	23	163	23	3	82	17	99.72	1.80
HA-38	24	Fsst	67.60	0.63	15.50	4.59	0.11	1.55	2.94	4.24	2.69	0.15	842	52	19	17	7	9	12	64	10.9	493	7.3	91	21	240	22	4	65	11	99.75	1.47
HA-50	45	Fsst	72.82	0.51	14.48	3.16	0.04	0.93	0.91	4.31	2.72	0.13	580	58	11	15	9	7	12	76	7.4	347	6.8	55	19	247	23	6	57	6	99.64	1.51
HA-59	53	Msst	60.10	1.04	16.88	7.35	0.13	2.74	4.15	4.09	3.25	0.27	890	58	43	18	9	16	14	74	18.1	895	7.8	145	25	217	22	9	107	18	99.28	2.44
HA-62	57	Vfsst	68.24	0.62	15.98	4.66	0.10	1.37	1.24	5.89	1.76	0.15	382	81	16	18	14	7	16	52	11.6	361	12.1	76	25	255	45	2	73	13	100.14	1.63
HA-72	76/6	Vfsst	67.38	0.57	15.65	3.87	0.08	1.26	2.80	3.79	4.41	0.18	733	76	4	17	12	3	21	120	9.6	591	9.1	53	26	279	29	7	79	4	99.82	2.43
HA-80	86	Fsst	74.99	0.55	15.21	1.20	0.08	0.37	0.31	5.40	1.76	0.13	505	51	22	16	9	4	10	59	5.9	348	6.4	44	20	220	17	3	68	5	99.98	1.49
HA-82	87	Fsst	68.85	0.85	17.31	3.43	0.05	0.64	0.50	5.46	2.67	0.23	575	52	82	19	10	11	23	87	12.9	362	5.1	95	19	255	19	21	63	9	99.52	2.46
Sandstone average			*68.62*	*0.62*	*15.43*	*4.22*	*0.08*	*1.40*	*2.36*	*4.28*	*2.83*	*0.16*	*726*	*59*	*22*	*18*	*10*	*8*	*15*	*84*	*11.4*	*408*	*8.6*	*78*	*23*	*232*	*25*	*6*	*73*	*10*	*99.75*	*1.93*

Table 1 (ctd). Whole-rock XRF major and trace element XRF analyses of sandstones and mudrocks from the Tsetserleg terrane, central Mongolia.

			Major elements (wt%)										Trace elements (ppm)																			
SaNr	Field No	Lith	SiO_2	TiO_2	Al_2O_3	Fe_2O_3	MnO	MgO	CaO	Na_2O	K_2O	P_2O_5	Ba	Ce	Cr	Ga	Nb	Ni	Pb	Rb	Sc	Sr	Th	V	Y	Zr	La	As	Zn	Cu	Total*	LOI
Tsetserleg Formation mudrocks																																
HA-58	52/1	Mst	65.53	0.66	17.13	5.07	0.08	1.59	1.85	3.56	4.35	0.17	896	78	19	21	16	7	24	134	9.8	359	12.6	75	28	293	39	6	119	8	99.86	2.87
HA-64	61/1	Zst	65.35	0.70	16.81	5.18	0.11	1.66	1.74	2.98	5.31	0.17	1138	62	18	22	13	10	12	165	11.0	443	12.3	90	24	238	33	3	91	36	99.50	2.70
HA-65	64/1	Mst	65.77	0.72	16.26	4.89	0.09	1.42	2.44	3.22	4.98	0.21	949	69	9	21	12	5	15	138	9.1	1282	11.8	79	25	268	27	1	64	12	99.40	1.60
HA-66	65/1	Zst	63.81	0.69	17.48	5.09	0.11	1.56	2.52	3.39	5.09	0.26	1152	76	10	23	12	5	15	139	10.8	1017	10.8	77	26	306	29	4	77	7	99.57	1.97
HA-67	70/1	Mst	64.50	0.74	17.31	5.32	0.09	1.65	2.18	3.24	4.79	0.19	969	81	9	22	15	8	17	132	9.9	592	10.9	88	27	316	38	3	83	9	99.74	2.08
HA-70	74/1	Zst	63.81	0.73	17.15	5.04	0.09	1.74	3.59	3.19	4.32	0.33	1016	83	16	23	13	7	25	117	11.1	567	10.6	87	30	288	45	8	70	13	99.73	1.86
HA-71	75/1	Mst	65.44	0.79	16.49	5.24	0.07	1.77	2.59	3.61	3.78	0.22	630	77	26	23	14	12	30	107	12.4	522	10.7	101	30	284	34	8	84	16	99.41	1.90
HA-75	78/1	Mst	63.14	0.65	16.81	4.67	0.10	1.44	3.90	3.90	5.07	0.32	1219	90	7	19	14	4	29	115	10.3	386	11.4	61	32	306	64	8	92	5	99.20	4.03
HA-76	79/1	Mst	69.65	0.57	14.35	4.04	0.08	1.26	2.90	3.52	3.50	0.13	767	74	6	17	8	3	22	98	8.5	393	8.1	56	19	257	36	8	75	30	99.44	3.39
HA-77	80/1	Mst	69.00	0.62	15.49	3.78	0.06	1.26	1.79	4.46	3.37	0.17	634	68	8	18	14	5	17	101	7.9	351	10.6	71	22	246	32	7	69	8	99.88	2.32
HA-84	88/1	Mst	66.24	0.72	16.77	5.42	0.07	1.52	1.05	4.08	3.91	0.21	850	60	19	19	14	5	20	126	10.4	388	9.9	90	23	281	30	11	92	25	99.43	2.63
HA-85	89/1	Mst	66.03	0.65	16.49	4.67	0.08	1.87	2.45	3.63	3.98	0.16	828	73	11	21	14	7	20	123	11.7	293	10.9	79	25	289	31	6	79	3	99.68	2.75
HA-97	100/1	Zst	63.99	0.82	17.52	5.44	0.07	2.47	1.77	3.21	4.48	0.22	851	74	18	24	17	13	30	177	10.9	350	13.7	97	32	213	41	12	99	22	99.90	3.04
HA-122	68/1	Mst	65.13	0.69	16.25	5.49	0.11	1.66	2.44	3.85	4.09	0.29	1029	71	10	20	13	4	18	98	10.1	487	10.8	80	26	283	38	8	84	18	99.28	2.29
HA-123	69/1	Mst	65.78	0.77	16.85	4.29	0.07	1.42	2.33	3.11	5.11	0.26	1037	93	18	22	13	9	20	133	10.1	580	10.8	91	32	293	41	5	71	10	98.92	1.68
Mudrock average			*65.54*	*0.70*	*16.61*	*4.91*	*0.08*	*1.62*	*2.37*	*3.53*	*4.41*	*0.22*	*931*	*75*	*14*	*21*	*13*	*7*	*21*	*127*	*10.3*	*534*	*11*	*82*	*27*	*277*	*37*	*6*	*83*	*15*	*99.53*	*2.47*
Tsetserleg Formation sandstones																																
HA-57	52	Msst	61.43	0.90	17.10	6.46	0.11	2.29	2.51	5.20	3.75	0.26	1088	56	28	19	9	11	14	77	13.4	680	8.6	115	24	220	27	7	99	7	99.24	1.83
HA-68	73	Csst	64.47	0.77	16.51	5.05	0.09	1.54	2.28	3.77	5.29	0.23	1756	46	9	20	11	5	17	128	10.6	674	7.0	83	22	227	26	4	84	7	99.97	1.57
HA-69	74	Msst	67.95	0.58	15.55	4.08	0.06	1.35	2.54	4.60	3.12	0.17	767	53	11	18	9	7	14	77	9.7	549	7.4	72	21	202	22	6	64	7	99.64	1.76
HA-78	80/2	Msst	71.00	0.22	17.27	1.48	0.01	0.49	0.28	5.76	3.37	0.11	602	21	2	23	5	2	31	99	3.1	307	3.6	9	3	123	2	9	72	4	99.58	1.28
HA-94	99	Csst	76.04	0.39	13.12	2.20	0.03	0.72	0.77	4.63	2.01	0.08	509	51	8	12	7	5	13	54	5.9	293	6.2	36	16	245	18	4	44	6	99.45	1.01
HA-95	99/1	Vfsst	68.03	0.69	17.11	4.48	0.04	1.44	1.19	2.93	3.92	0.18	718	62	20	21	13	10	18	124	12.2	256	10.0	91	26	230	31	12	89	15	99.24	2.56
HA-120	67	Msst	67.68	0.64	16.28	4.36	0.05	1.47	1.68	3.45	4.22	0.17	867	73	14	20	12	7	21	134	9.4	469	11.2	83	25	271	28	7	85	11	99.22	1.66
HA-121	68	Msst	61.68	0.88	18.27	5.78	0.10	1.78	1.64	5.20	4.41	0.26	1349	60	15	19	14	6	25	98	12.0	413	11.1	100	29	270	27	9	99	3	99.55	1.89
HA-124	71	Msst	65.83	0.80	15.73	5.31	0.08	1.66	3.33	4.05	2.97	0.22	844	64	12	21	11	4	15	77	9.5	514	7.7	94	22	214	32	5	82	9	99.15	1.76
HA-125	73/2	Csst	64.66	0.79	16.18	5.47	0.09	1.60	3.21	3.40	4.37	0.22	1165	64	19	22	12	7	17	106	15.3	818	9.8	97	25	258	28	6	87	11	99.62	1.63
HA-126	75	Msst	67.83	0.62	15.79	4.37	0.06	1.32	1.79	4.28	3.78	0.15	943	66	17	17	9	6	16	89	8.5	426	7.5	76	21	262	26	5	69	10	99.20	1.30
Sandstone average			*66.96*	*0.66*	*16.27*	*4.46*	*0.07*	*1.42*	*1.93*	*4.30*	*3.75*	*0.19*	*964*	*56*	*14*	*19*	*10*	*6*	*18*	*97*	*10.0*	*491*	*8*	*78*	*21*	*229*	*24*	*7*	*79*	*8*	*99.44*	*1.66*
Jargalant Formation mudrocks																																
HA-44	33/1	Mst	64.73	0.61	17.60	4.27	0.08	1.13	1.45	5.26	4.73	0.14	995	95	2	25	18	2	24	156	8.2	338	11.1	45	28	368	48	4	101	2	99.42	1.17
HA-45	38	Zst	66.05	0.63	16.37	4.15	0.07	1.26	2.19	3.55	5.54	0.18	1570	50	2	20	11	1	31	135	9.0	1127	10.0	61	20	283	23	4	87	6	99.17	0.94
HA-47	39/1	Mst	65.79	0.75	17.77	4.82	0.07	1.44	0.63	4.03	4.40	0.31	1052	60	11	22	16	5	10	131	9.0	416	13.4	88	20	286	40	18	98	9	99.75	1.69
HA-48	40/1	Mst	72.08	0.29	15.29	2.31	0.06	0.69	2.38	4.41	2.41	0.09	474	37	1	15	6	1	13	98	5.0	248	9.4	19	14	158	21	1	45	1	99.71	2.91
HA-86	92/1	Zst	65.87	0.80	17.84	5.35	0.05	1.64	1.06	3.12	4.04	0.23	874	74	25	23	16	12	19	121	10.5	221	13.5	112	30	277	40	10	114	6	99.70	3.67
HA-88	93/1	Mst	66.02	0.72	17.67	4.63	0.08	1.42	0.80	3.44	5.02	0.20	1009	75	19	22	14	10	16	152	8.1	288	13.9	97	31	264	40	16	110	9	99.29	2.86
HA-90	94/1	Mst	69.26	0.68	15.53	4.30	0.05	1.47	1.47	4.20	2.82	0.21	622	68	16	18	13	8	23	84	11.4	330	11.6	80	26	219	31	7	84	9	99.09	1.84
HA-93	96/1	Zst	66.48	0.65	16.21	5.09	0.07	1.75	1.95	4.12	3.51	0.18	880	59	22	20	12	10	23	106	10.0	393	10.9	91	25	258	33	16	98	19	99.48	0.88
Mudrock average			*67.03*	*0.64*	*16.78*	*4.36*	*0.07*	*1.35*	*1.49*	*4.02*	*4.06*	*0.19*	*934*	*65*	*12*	*20*	*13*	*6*	*20*	*123*	*8.9*	*420*	*12*	*74*	*24*	*264*	*34*	*10*	*92*	*8*	*99.45*	*2.00*
Jargalant Formation sandstones																																
HA-43	33	Msst	66.93	0.59	16.76	3.88	0.08	0.99	1.72	5.59	3.28	0.17	867	90	5	19	17	2	25	87	7.8	400	11.7	44	25	322	38	6	83	5	99.77	1.34
HA-46	39	Fsst	56.77	0.79	17.46	5.13	0.18	1.61	8.33	5.64	3.72	0.37	945	71	10	20	10	4	20	90	13.3	755	10.6	81	24	264	32	4	80	3	99.46	6.14
HA-87	93	Msst	75.66	0.43	13.20	2.51	0.03	0.77	0.48	3.60	3.20	0.12	692	58	9	14	9	4	9	88	4.7	293	8.4	46	18	250	25	11	52	39	99.07	1.50
HA-89	94	Csst	66.16	0.68	16.76	4.87	0.06	1.44	2.23	3.45	4.15	0.20	1061	66	10	19	12	6	21	117	10.8	466	10.9	76	23	256	36	7	89	10	99.75	2.47
HA-91	95	Csst	64.69	0.84	17.03	5.27	0.07	1.46	1.08	5.64	3.62	0.29	886	64	20	21	17	10	23	85	11.3	362	18.1	92	29	283	28	2	111	14	99.85	2.24
HA-92	96	Msst	72.20	0.51	14.20	4.09	0.05	1.31	1.50	3.07	2.94	0.14	544	62	13	16	9	10	20	87	9.1	308	7.9	61	20	231	25	4	73	26	99.53	1.29
Sandstone average			*67.07*	*0.64*	*15.90*	*4.29*	*0.08*	*1.26*	*2.56*	*4.50*	*3.49*	*0.21*	*833*	*68*	*11*	*18*	*12*	*6*	*20*	*92*	*9.5*	*430*	*11*	*67*	*23*	*268*	*31*	*6*	*81*	*16*	*99.57*	*2.50*

Footnotes: 1. Abbreviations: SaNr = sample number; Field No. = Field number; Lith = Lithology (csst, msst, fsst, vfsst = coarse, medium, fine and very fine-grained sandstone, respectively; zst = siltstone; mst = mudstone; LOI = loss on ignition.

Total* = original "as analyzed" analytical total, on an anhydrous (ignited) basis. Total iron expressed as Fe2O3.

2. NOTE: data are tabulated on a 100% normalized basis. The normalizing factors for the major elements were also applied to the trace element data. Conventional hydous analyses can be calculated if desired, using the listed Total* and LOI values.

wt% (Table 1). Average SiO_2 contents of the sandstones are remarkably uniform, decreasing only slightly from the oldest Erdenetsogt Formation (68.62 wt%) to the younger Tsetserleg (66.96 wt%) and Jargalant Formations (67.07 wt%). Average SiO_2 contents in the mudrocks are equally uniform, at 65.56, 65.54, and 67.03 wt%, respectively (Table 1). Average Al_2O_3 contents in Erdenetsogt (17.25 wt%), Tsetserleg (16.61 wt%) and Jargalant (16.78 wt%) mudrocks also show little variation. All the mudrock averages are, however, slightly greater than those for companion sandstones (15.43, 16.27, and 15.90 wt%, respectively).

The small contrasts in SiO_2 and Al_2O_3 between formations and lithotypes and lack of consistent trend by age suggest that contrasts between the other major elements should also be limited. At first sight this is the case, but closer examination of the data shows some trends. For Fe_2O_3 and MgO, average contents in the mudrocks are consistently a little greater than in companion sandstones (Table 1). Furthermore, average contents of both elements in the mudrocks decrease from Erdenetsogt through Tsetserleg to Jargalant Formation; for MgO the respective averages are 1.67, 1.62, and 1.35 wt%, and for Fe_2O_3 5.30, 4.91, and 4.36 wt%. This pattern is not repeated in the sandstones, with slightly higher averages for both elements in the Tsetserleg Formation. Average TiO_2 content also decreases in the mudrocks (0.72, 0.70, 0.64 wt%, respectively), and contents are higher than in the sandstones in all except the Jargalant Formation, where sandstones and mudrocks both average 0.64 wt%. The range in averages of the minor elements MnO and P_2O_5 are very small (0.07-0.08 and 0.15-0.21 wt%, respectively), and show no clear trend with lithotype or age.

The more mobile major elements CaO, Na_2O and K_2O show variable patterns (Table 1). Average CaO contents show no clear trend. Average abundance in the Tsetserleg mudrocks (2.37 wt%) is greater than in Erdenetsogt (1.75 wt%) and Jargalant (1.49 wt%) mudrocks, whereas Tsetserleg sandstones average less (1.93 wt%) than their Erdenetsogt and Jargalant equivalents (2.36 and 2.56 wt%, respectively). K_2O contents also show no trend with age, with higher lithotype averages in the Tsetserleg Formation (4.41 wt% in mudrocks, 3.75 wt% for sandstones) than in equivalents in the other two units. However, in all three formations, average K_2O abundances in the mudrocks are significantly greater than in companion sandstones, especially in the older units. The clearest trends, however, are shown by Na_2O. Average abundances increase in both lithotypes from Erdenetsogt through Tsetserleg to Jargalant Formation, with values of 3.09, 3.53, and 4.02 wt% in mudrocks, respectively, and 4.28, 4.30, and 4.50 wt% in sandstones. Furthermore, in each formation, the sandstone average is greater than that for the mudrocks, especially in the Erdenetsogt and Tsetserleg Formations, where the contrast is near 1 wt%, representing enrichment in the sandstones of about one third of the amount present in the mudrocks. The above trends for the major elements suggest some contrasts in composition and hence provenance or diagenetic history occur between the formations.

The mobile large ion lithophile elements (LILE) Ba and Sr are the most abundant of the trace elements, with ranges of averages of 726-964 and 342-534 ppm respectively (Table 1). Average Rb abundances are also relatively high (84-131 ppm). For Ba and Sr there is no pattern by lithotype or age, with highest averages for both elements in the Tsetserleg Formation. Although Rb contents show virtually no contrast by age (average 131, 127, 123 ppm in mudrocks by formation, respectively; 84, 97, 92 ppm in sandstones), the mudrocks are consistently enriched relative to the sandstones in each formation, paralleling the pattern seen for K_2O.

A second group of highly-charged elements that are typically immobile in surface conditions (Ce, La, Nb, Th, Y, Zr) show common behaviour. Although average concentrations do not vary systematically with age (most show highest values in the Tsetserleg Formation), within each formation the mudrocks are enriched relative to the companion sandstones, often by more than 10% of the amount present. This suggests association with the clay fraction or silt-sized heavy minerals including zircon, monazite, or apatite).

Four ferromagnesian trace elements (Cr, Ni, V, Sc) show a similar pattern, with average abundances higher in mudrocks than in sandstones in each formation. Concentrations within each lithotype also tend to decrease with age, although the contrasts are small for all except vanadium, the most abundant element in the group (averaging 67-93 ppm). The chalcophile elements analyzed (Cu, Zn, As, Pb) also tend to be enriched in mudrocks relative to the sandstones on average, but show variable behaviour with age, tending to have slightly higher concentrations in the Tsetserleg Formation.

Overall, the results above show that the average abundances of some elements vary with lithotype and age, despite the relatively small variation seen in average SiO_2 and Al_2O_3 contents between lithotype and formation. The cause of these variations and their implications will be investigated in future work.

Conclusions

This study reports new whole-rock analyses of 94 sandstones and mudrocks from the Erdenetsogt, Tsetserleg and Jargalant Formations of the Tsetserleg terrane of the Hangay sub-belt of central Mongolia. Average elemental abundances show some contrast between lithotype and formation, suggesting subtle changes in provenance, sorting, source weathering, tectonic setting and diagenesis within this terrane. These factors will be addressed in future work in an effort to clarify the controversial origin of the Hangay-Hentey basin, based on geochemical proxies.

Acknowledgements

The late Professor Serjkhuu Dandar of the School of the Geology and Petroleum Engineering of the Mongolian University of Science and Technology provided invaluable assistance during our field survey, and made many helpful suggestions for our study. Without his contribution this work would have been impossible. We also thank Professor Genden Ukhnaa for his support with sample storage and transportation.

References

Badarch, G., 2005, Tectonic overview of Mongolia. *Mongolian Geoscientist*, **27**, 1-7.

Badarch, G., Cunningham, D.W. and Windley B. F., 2002, A new terrane subdivision for Mongolia: implication for the Phanerozoic crustal growth of Central Asia. *Journal of Asian Earth Sciences*, **21**, 87-110.

Bhatia, M.R. and Crook, K.A.W., 1986, Trace element characteristics of greywackes and tectonic setting discrimination of sedimentary basins. *Contributions to Mineralogy and Petrology*, **92**, 181-193.

Bayamba, J., Ichinnorov, N., Minjin, Ch., Sodov, J., Sersmaa, G., Tungalag, Ts. and Uranbileg, L., 1994, Mongolian Stratigraphy Dictionary. Ulaanbaatar, Mongolia, 233p.

Dobretsov, N.L., Buslov, M.M., Delvaux, D., Berzin, N.A. and Ermikov, V.D., 1996, Meso-and Cenozoic tectonics of Central Asian Mountain Belt: Effects of lithospheric plate Interaction and mantle plumes. *International Geology Review*, **38**, 430-466.

Genden, U., Serjkhuu, D. and Purevjav, N., 2005, Exploration report-1. Gold mineralization examination on the Sudut mining area. *School of Geology and Petroleum Engineering, Ulaanbaatar.*

Genden, U., Sereenen, J. and Purevjav, N., 2007, Geology and gold mineralization at Zuun Sodot placer area, central Mongolia. *Journal of Mongolian Geology,* **17**, 89-92.

Jahn, B.M., Wu, F. and Chen, B., 2000, Granitoids of Central Asian Orogenic Belt and continental growth in the Phanerozoic. *Transactions of the Royal Society of Edinburgh, Earth Science*, **91**, 181-193.

Jahn, B., Capdevila, R., Liu, D., Vernon, A. and Badarch, G., 2004, Sources of Phanerozoic granitoids in the transect Bayanhongor-Ulaanbaatar, Mongolia: geochemical and Nb isotopic evidence, and implications for Phanerozoic crustal growth. *Journal of Asian Earth Sciences,* **23**, 629-653.

Kashiwagi, K., Tsukada, K. and Bodonchuud, C.M., 2004, Paleozoic spherical radiolarians from the Gorkhi Formation, southwest Khentei range, central Mongolia; a preliminary report. *Mongolian Geoscientist,* **24**, 15-24.

Kelty, K.T., Yin An., Dash. B., Gehrels, G.E. and Ribeiro, A.E., 2008, Detrital-zircon geochronology of Paleozoic sedimentary rocks in the Hangay-Hentey basin, north-central Mongolia: Implication for the tectonic evolution of the Mongol-Okhotsk Ocean in central Asia. *Tectonophysics*, **451**, 290-311.

Kimura, J. I. and Yamada, Y., 1996, Evaluation of major and trace element XRF analyses using a flux to sample ratio of two one-glass beads. *Journal of Mineralogy, Petrology and Economic Geology*, **91**, 62-72.

Kröner, A., Windley, B.F., Badarch, G., Tomurtogoo, O., Hegner, E., Jahn, B.M., Gruschka, S., Khain, E.V., Demoux, A. and Wingate, M.T.D., 2007, Accretionary growth and crust formation in the central Asian Orogenic Belt and comparison with Arabian-Nubian shield. *Memoirs of the Geological Society of America,* **200**, 181-209.

Kurihara, T., Tsukada, K., Otoh, S., Kashiwagi, K., Minjin, Ch., Dorjsuren, B., Bujinlkham, B., Sermaa, G., Manchuk, N., Niwa, M., Tokiwa, T., Hikichi, G. and Kozuka, T., 2009, Upper Silurian and Devonian pelagic deep-water radiolarian chert from the Khangai-Khentei belt of Central Mongolia: Evidence for Middle Paleozoic subduction-accretion activity in the Central Asian Orogenic Belt. *Journal of Asian Earth Sciences*, **34**, 209-225.

Lehman, J., Schulmann, K., Lexa, O., Corsini, M., Kröner, A., Stipska, P., Tomurhuu, D. and Otgonbator, D., 2010, Structural constraints on the evolution of the Central Asin Orogenic Belt in SW Mongolia. *American Journal of Science*, **310**, 575-628.

Long, X.P., Yuan, C., Sun, M., Xiao, W., Zhao, G., Wang, Y. and Cai, Y., 2010, Detrital zircon U-Pb ages and Hf isotopes of the Early Paleozoic flysch sequence in the Chinese Altai, NW China: new constraints on depositional age, provenance and tectonic evolution. *Tectonophysics*, **480**, 213-231.

Long, X.P., Yuan, C., Sun, M., Xiao, W., Wang, Y., Cai, K. and Jiang, Y., 2011a, Geochemistry and Nd isotopic composition of the Early Paleozoic flysch sequence in the Chinese Altai, Central Asia: Evidence for a northward-derived mafic source and insight into Nd model ages in accretionary orogen. *Gondwana Research*, **19**, (*in press*) doi:10.1016/j.gr.2011.04.009.

Long, X.P., Yuan, C., Sun, M., Safonova, I., Xiao, W. and Wang, Y., 2011b, Geochemistry and U-Pb detrital zircon dating of Paleozoic graywackes in East Junggar, NW China: Insights into subduction-accretion processes in the southern Central Asian Orogenic Belt. *Gondwana Research,* **19**, (*in press*) doi:10.1016/j.gr.2011.05.015.

Orolmaa, O., Erdenesaihan, G., Borisenko, A.S., Fedoseev, G.S., Badich, V.V. and Zhmodik, S.M., 2008, Permian-Triassic granitoid magmatism and metallogeny of the Hangayn (central Mongolia). *Russian Geology and Geophysics,* **49,** 534-544.

Purevjav, N. and Roser, B.P., 2011, Preliminary geochemical characterization of Tsetserleg terrane sedimentary rocks in the western Hangay basin, Mongolia. *Proceedings of the International Conference on Knowledge Based Industry, ICKI 2011,* July 6-7, 2011, Ulaanbaatar, Mongolia, 473-477.

Ren, R., Han, B., Ji, J., Zhang, L. and Su, L., 2011, U-Pb age detrital zircons from the Tekes River, Xinjiang, China, and implications for tectonomagmatic evolution of the South Tian Shan Orogen. *Gondwana Research,* **19***,* 460-470.

Rojas-Agramonte, Y., Kröner, A., Demoux, A., Xia, X., Wang, W., Donskaya, T., Liu, D. and Sun, M., 2011, Detrital and xenocrystic zircon ages from Neoproterozoic to Paleozoic arc terranes of Mongolia: Significance for the origin of crustal fragments in the Central Asian Orogenic Belt. *Gondwana Research*, **19**, 751-763.

Roser, B.P. and Korsch R.J., 1986. Determination of tectonic setting of sandstone and mudstone suites using SiO_2 and K_2O/Na_2O ratio. *Journal of Geology*, **94**, 635-650.

Roser, B.P., Sawada, Y. and Kabeto, K., 1998, Crushing performance and contamination trials of a tungsten carbide ring mill compared to agate grinding. *Geoscience Reports of Shimane University*, **17**, 1-9.

Roser, B.P., Kimura, J.-I. and Hisatomi, K., 2000, Whole-rock elemental abundances in sandstones and mudrocks from the Tanabe Group, Kii Peninsula, Japan. *Geoscience Reports of Shimane University,* **19**, 101-112.

Roser, B.P., Kimura, J. and Sifeta, K., 2003, Tantalum and niobium contamination from tungsten carbide ring mills: much ado about nothing. *Geoscience Reports of Shimane University*, **22**, 107-110.

Ruzhentsev, S.V. and Mossakovskiv, A.A., 1996, Geodynamic and tectonic evolution of the Central Asian Paleozoic structure as the result of the interaction between the Pacific and Indo-Atlantic segments of the earth. *Geotectonics*, **29**, 211-311.

Sambuu, O. and Ishihara, S., 2005, Paleozoic and Mesozoic granitic rocks in the Hotont area, central Mongolia. *Bulletin of the Geological Survey of Japan*, **56**, 245-258.

Sengör, A.M.C. and Natal'in, B.A., 1996, Paleotectonics of Asia: Fragments of a synthesis. In: The Tectonic Evolution of Asian (eds Yin, A. and Harrison, M.). *Cambridge University Press*, p. 486-640.

Sengör, A.M.C., Natal'in, B.A. and Burtman, V.S., 1993, Evolution of the Altaid tectonic collage and Paleozoic crustal growth in Eurasia. *Nature*, **364**, 269-307.

Tomurtogoo, O., 1997, A new tectonic scheme of the Paleozoides in Mongolia. *Mongolian Geoscientist,* **14**, 12-18.

Tomurtogoo, O., Tomurkhuu, D., Erdenesaikhan, G., Kröner, A., Demoux,

A., and Rojas-Agramonte, Y., 2006, Excursion in the Central and Southern Mongolia. *In* Tomurhuu, D., Natal'in, B., Ariunchimeg, Y., Khishigsuren, S., and Erdenesaikhan, G. (eds), Second International Workshop and Field Excursions for IGCP Project-480. *Structural and Tectonic Correlation across the Central Asian Orogenic Collage: Implications for Continental Growth and Intracontinental Deformation*. Abstracts and Excursion Guidebook: Ulaanbaatar, Institute of Geology and Mineral Recourses, Mongolian Academy of Sciences, p. 107-146.
Wainwright, A.J., Tosdal, R.M., Wooden, J.I., Mazdab, F.K. and Friedman, R.M., 2011, U-Pb (zircon) geochemical constraints on the age, origin, and evolution of Paleozoic arc magmas in the Oyu Tolgoi porphyry Cu-Au district, southern Mongolia. *Gondwana Research*, **19**, 764-787.
Windley, B.F., Alexeiev, D., Xiao, W., Kröner, A. and Badarch, G., 2007, Tectonic model for accretion of the Central Asian Orogenic Belt. *Journal of the Geological Society* (*London*), **164**, 31-47.

(Received: Oct. 3, 2011, Accepted: Oct. 28, 2011)